

Original Paper

Effect of Mercury on Membrane Proteins, Anionic Transport and Cell Morphology in Human Erythrocytes

Rosaria Notariale^a Emmanuel Längst^b Pasquale Perrone^a David Crettaz^b
Michel Prudent^{b,c,d} Caterina Manna^a

^aDepartment of Precision Medicine, School of Medicine, University of Campania "Luigi Vanvitelli", Naples, Italy, ^bLaboratoire de Recherche sur les Produits Sanguins, Innovation et Produits Thérapeutiques, Transfusion Interrégionale CRS, Epalinges, Switzerland, ^cCenter for Research and Innovation in Clinical Pharmaceutical Sciences, Institute of Pharmaceutical Sciences of Western Switzerland, University Hospital and University of Lausanne, Lausanne, Switzerland, ^dInstitute of Pharmaceutical Sciences of Western Switzerland, University of Geneva, University of Lausanne, Lausanne, Switzerland

Key Words

Ankyrin • Anionic transport • Erythrocytes • Flotillin-2 • Mercury

Abstract

Background/Aims: Mercury (Hg) is a heavy metal widespread in all environmental compartments as one of the most hazardous pollutants. Human exposure to this natural element is detrimental for several cellular types including erythrocytes (RBC) that accumulate Hg mainly bound to the SH groups of different cellular components, including protein cysteine residues. The cellular membrane represents a major target of Hg-induced damage in RBC with loss of physiological phospholipid asymmetry, due to phosphatidylserine (PS) exposure to the external membrane leaflet. To investigate Hg-induced cytotoxicity at the molecular level, the possible interaction of this heavy metal with RBC membrane proteins was investigated. Furthermore, Hg-induced alterations in band 3 protein (B3p) transport function, PS-exposing macrovesicle (MVs) formation and morphological changes were assessed. **Methods:** For this aim, human RBC were treated *in vitro* with different HgCl₂ concentrations (range 10-40 μM) and the electrophoretic profile of membrane proteins as well as the expression levels of Ankyrin and Flotillin-2 evaluated by SDS-PAGE and Western blot, respectively. The effect of alterations in these proteins on RBC morphology was evaluated by digital holographic microscopy and anionic transport efficiency of B3p was evaluated as sulphate uptake. Finally, PS-bearing MVs were quantified by annexin-V binding using FACS analysis. **Results:** Findings presented in this paper indicate that RBC exposure to HgCl₂ induces modifications in the electrophoretic profile of membrane protein fraction. Furthermore, our study reveals the Hg induced alterations of specific membrane proteins, such as Ankyrin, a protein essential for membrane-cytoskeleton linkage and Flotillin-2, a major integral protein of RBC lipid rafts, likely responsible for decreased

membrane stability and increased fragmentations. Accordingly, under the same experimental conditions, RBC morphological changes and PS-bearing MVs release are observed. Finally, RBC treatment significantly affects the B3p-mediated anionic transport, that we report reduced upon HgCl_2 treatment in a dose dependent manner. **Conclusion:** Altogether, the findings reported in this paper confirm that RBC are particularly vulnerable to Hg toxic effect and provide new insight in the Hg-induced protein modification in human RBC affecting the complex biological system of cellular membrane. In particular, Hg could induce dismantle of vertical cohesion between the plasma membrane and cytoskeleton as well as destabilization of lateral linkages of functional domains. Consequently, decreased membrane deformability could impair RBC capacity to deal with the shear forces in the circulation increasing membrane fragmentations. Furthermore, findings described in this paper have also significant implication in RBC physiology, particularly related to gas exchanges.

© 2022 The Author(s). Published by
Cell Physiol Biochem Press GmbH&Co. KG

Introduction

Mercury (Hg) is a heavy metal classified as one of the most hazardous global pollutants [1, 2], exerting its toxic effects even at trace amounts. Hg contamination, indeed, is extensive in all environmental compartments such as soil, air, and water. It reacts adversely within organisms and bioaccumulates in aquatic animal tissue. The consumption of contaminated fish, indeed, represents the major Hg route of human exposure [3]. In particular, the average blood mercury level of consumers of high-fish diets was 3.7 times higher than those observed in those who reported consuming no fish [4]. This natural element can exist in different redox forms (elemental, inorganic and organic), each with a different pathway of exposure and a unique toxicological profile [5]. Hg reacts with high affinity to SH groups and therefore binds a variety of cellular components, but mechanisms underlying its cytotoxicity turn out to be very complex and not yet fully understood [6]. Overall, Hg poisoning in humans manifests as neurological, kidney, immune, and respiratory disorders, associated with imbalances in calcium homeostasis, stimulation of apoptosis, and alterations in the antioxidant defense system [7–10].

A growing body of evidence suggests that Hg exposure may lead to adverse effects on cardiovascular tissues [11]. Several experimental evidence indicate that cardiac function is directly affected by Hg exposure. Specifically, high levels of Hg can induce alterations in heart function through dysregulation of humoral and neuronal modulation, alterations in innervation, or alterations in blood vessels, resulting in decreased cardiac excitability and contractility [12, 13]. Furthermore, there is an increasing body of data associating Hg exposure and endothelium dysfunction. In this respect, workers occupationally exposed to Hg vapor show increased blood concentration of this heavy metal, associated with significant alterations in the coagulation system [14]. Accordingly, Hg intoxication is associated with an increased risk of cardiovascular diseases (CVD) [15–17].

Regardless of the route of absorption, Hg finds its way through blood stream allowing its distribution to tissues and organs. Among blood cells, human erythrocytes (RBC) are an important target of Hg toxicity because this metal ion preferentially accumulates in these cells, reaching concentrations higher than those found in plasma [18, 19]. Indeed, the highest blood mercury concentrations reported in humans were in gold mine workers in the Amazon area, whose blood mercury levels reached $150 \mu\text{g/L}$ ($\sim 0.75 \mu\text{M}$), in contrast to the average plasma levels of around $83.3 \mu\text{g/L}$ ($0.4 \mu\text{M}$) [14, 20].

In recent years, particular attention has been focused on the mechanisms promoting vascular dysfunction and thrombotic events as a consequence of Hg-induced RBC damage [21, 22]. We recently reviewed the Hg-induced metabolic and morphological alterations that could affect RBC physiology, responsible for activation of a pro-thrombotic activity and likely acting as a major player in endothelial dysfunction [15]. Among these alterations, loss of physiological membrane asymmetry, due to phosphatidylserine (PS) exposure, is

proved to enhance RBC adhesion to endothelial cells and clot formation [19]. Alterations in RBC membrane proteins, including cytoskeleton proteins and Band 3 (B3p), the most abundant integral protein on the membrane, have also been reported to be prothrombotic factors [23]. In particular, modification of these proteins results in morphological changes and microvesicles (MVs) generation [24, 25] that are known to contribute to thrombotic events [26]. All together, these effects design RBC as an active contributor to vascular dysfunction associated with Hg intoxication.

A preliminary study from our group indicated that Hg exposure induces RBC membrane protein alterations [27]. To investigate Hg-induced cytotoxicity at the molecular level, the possible interaction of this heavy metal with specific membrane proteins was investigated. For this aim, human RBC were treated *in vitro* with different HgCl₂ concentrations (range 10-40 µM) and the electrophoretic profile of membrane proteins as well as the expression levels of Ankyrin, a protein essential for membrane-cytoskeleton linkage and Flotillin-2, a major integral protein of RBC lipid rafts [28, 29], were evaluated. Furthermore, Hg-induced alterations in B3p transport function, PS-exposing MVs and RBC morphological changes were assessed.

Materials and Methods

Chemicals and solutions

DIDS (4,40-diisothiocyanato-stilbene-2, 20-disulfonate), deoxycholic acid (DC), ponceau S and HgCl₂ were from Sigma Chemical Co. Bromophenol blue and Coomassie Brilliant Blue R-250 were purchased from Fluka Chemie, Buchs, Switzerland. Tween-20 was bought from Roche Diagnostics (Mannheim, Germany), PBS 10x (1x PBS eq. to 137 mM NaCl, 2.7 mM KCl, 8.1 mM Na₂HPO₄ and 1.8 mM KH₂PO₄) from Laboratorium Dr. G. Bichsel (Interlaken, Switzerland), EDTA from Merck (MSD Merck Sharp & Dohme, Luzern, Switzerland), Tris-HCl from BIO-RAD (Hercules, CA, United States), ethanol from Thommen-Furler AG (Rüti bei Büren, Switzerland), SureBlock from Lubio Science (Luzern, Switzerland), BenchMark Protein Ladder (pre-stained or not) from Invitrogen (Carlsbad, CA, United States). Furthermore, Ankyrin B (2.20): sc-12718 and Flotillin-2 (Santa Cruz Biotechnology) as well as Annexin V-fluorescein isothiocyanate (V-FITC) Apoptosis Detection Kit (556547, BD Pharmingen, Franklin Lakes, NJ, USA) were used. DIDS was prepared in DMSO and diluted from 10 mM or 100 mM stock solution. Preparation of RBC and treatment with HgCl₂.

Whole blood was obtained with informed consent from healthy donors at Transfusion Interrégionale CRS (Epalinges, Switzerland) and RBC concentrates were prepared using a top-bottom bag system and mixed with saline adenine glucose mannitol solution for storage, as previously described [30]. It was collected in tubes and centrifuged at 2,000 g for 10 min at 4 °C. The RBC fraction was washed twice with isotonic saline solution (0.9 % NaCl) and resuspended in Krebs solution (pH 7.4) containing (mM) NaCl 125, KCl 4, MgSO₄ 1, Hepes 32, CaCl₂ 1, glucose 2.8, to obtain a 10 % (v/v) hematocrit (or 3% for the sulphate transport measurement). RBC were co-incubated at 37 °C for 4 h (only for sulphate transport measurement) or 24 h with HgCl₂ (10, 20, 40 µM).

Preparation of erythrocyte membranes

After HgCl₂ treatment, RBC were washed twice in 0.9 % NaCl (2 v) and centrifuged at 2,000 g for 10 min at 4 °C. Samples were lysed by incubation for 1 h at 4 °C in a hypotonic solution of 0.1x PBS under agitation (4 v of 0.1x PBS per 1 v of RBC pellet).

Membranes were separated by ultracentrifugation at 21,500 g, 75 min, 4 °C, to separate intracellular contents from membranes. We separated the supernatant, which contains the cytosolic fraction, from the lower part containing the membranes. The latter was washed 8 times (centrifugation at 21,500 g, 30 min, 4 °C) to remove as much as possible hemoglobin (Hb) from membranes. RBC membranes were stored at -80 °C until protein extraction [31].

Protein extraction

Thawed samples were centrifuged (21,500 g, 30 min, 4 °C). Subsequently, total membrane proteins were extracted under native conditions from pelleted membranes with DC buffer: 1 % DC in 50 mM Tris-HCl,

150 mM NaCl, pH 8.1. A final centrifugation was performed at 21,500 *g*, 30 min, 4 °C. Protein concentration of the supernatant, containing membrane proteins and cytoskeleton and were quantified using a nanodrop 2000c (Thermo scientific) [32].

SDS-PAGE analyses

Total membrane protein extracts were analyzed by SDS-PAGE. Ten µg of proteins from each sample and 3 µL of BenchMark Protein Ladder (or 10 µL of BenchMark Prestained Protein Ladder for Western blot, WB) were loaded on gels (Mini- PROTEAN TGX gels, 4–15%, BIO-RAD, United States). Following separation, proteins were stained with Coomassie Brilliant Blue R250 and acquired using a GelDoc system via Quantity One v.4.4.0 software (BIO-RAD, Hercules, CA, USA). The densitometric analysis of gel bands was carried out using the software ImageJ (Rasband, W.S., ImageJ, U.S. National Institute of Health, Bethesda, Maryland, USA, <https://imagej.nih.gov/>).

Western blotting

The WB analyses were performed on PVDF membranes (transfer 1 h at 100 V in Tris-Glycine buffer inside a Mini Trans-Blot Electrophoretic Transfer cell).

Membranes were rinsed in TBS-T (1x TBS, 0.05 % Tween-20) and blocked with SureBlock buffer (4 % in TBS-T) during 1 h at RT under agitation. Then, the membranes were washed 3 x 5 min in TBS-T. Blots were incubated overnight at 4 °C under agitation with the primary antibody (Ankyrin B 1/200 and Flotillin-2 1/6,000 in SureBlock buffer). After a quick rinse and washes of 3 x 5 min at RT in TBS-T, the membranes were re-incubated in SureBlock buffer for 30 min at RT under agitation.

Subsequently, membranes were incubated with the secondary antibody (Polyclonal goat anti-mouse immunoglobulins HRP, Dako, Denmark) diluted at 1/10,000 in SureBlock buffer, for 1 h at RT under agitation. The membranes were finally washed several times in TBS-T at RT under agitation.

The ECL reaction was achieved using the ECL Western blotting detection reagents (GE Healthcare, Little Chalfont, Buckinghamshire, United Kingdom) 1 min and the images were acquired by means of ImageQuant LAS 500 (GE healthcare, Uppsala, Sweden).

After the ECL reaction, the blots were rinsed and washed 3 x 5 min in TBS-T and then stripped for 40 min at RT under agitation in 20 mL of Restore™ Western Blot Stripping Buffer (Thermo Scientific, Rockford, IL, United States). Then, the blots were rinsed and washed again 3 x 5 min in TBS-T before a new blocking for 20 min at RT under agitation in SureBlock buffer. Finally, they were rinsed, washed 2 x 5 min in TBS-T and stored at 4 °C for further immunodetection. Bands of interest were quantified by densitometry of the ImageJ software (1.51w1) and expressed as "volume". The data were then corrected by the total protein loading detected on Ponceau S by densitometry. The relative volumes were calculated as follows:

$$\text{Relative Volume}_{\text{Protein}} = \text{Volume}_{\text{Protein,ECL}} / \text{Volume}_{\text{Whole proteins,Ponceau}}$$

where $\text{Volume}_{\text{Protein,ECL}}$ is the band volume of the protein of interest from WB and $\text{Volume}_{\text{Whole proteins,Ponceau}}$ is the amount of loaded proteins determined by the densitometry analyses of whole lane from Ponceau red-stained membrane [32].

Sulphate transport measurement

According to Romano and Passow [33], samples were suspended in an isotonic medium (in mM: 118 Na₂SO₄, 10 HEPES, 5 glucose, pH 7.4) at a hematocrit of 3%, and centrifuged for 5 minutes at 1,000*g*. After 15, 30, 45 and 60 minutes of incubation at 37 °C with or without (control) HgCl₂ (10-40 µM), 5µM of DIDS stopping medium was added at different intervals to 500 µL of samples and kept on ice. The presence of DIDS, a compound that binds irreversibly and specifically to the extracellular moiety of the integral membrane B3p, inhibits SO₄²⁻ transport in RBC [34].

After the last sample withdrawal, RBC were washed two times in cold isotonic solution (in mM: 150 NaCl, 20 HEPES, pH 7.4) at 4 °C, 1000 *g*, 5 min to remove SO₄²⁻ from the external medium and hemolyzed in 1 mL of distilled water, while proteins were hydrolyzed by perchloric acid (4 % v/v).

The membranes were then discarded by pelleting them with a 10 min centrifugation at 4,000 *g* at 4 °C. Sulphate ions in the supernatant were precipitated by sequentially adding and mixing 1 mL of a glycerol-distilled-water solution (1:1), 1 mL of a NaCl-HCl (4 M and 37%, respectively) solution (12:1) and 500 µL of 1.24 M BaCl₂ · x 2H₂O, to obtain a homogeneous barium sulphate precipitate. The intracellular sulphate

concentration was measured by atomic absorption spectrophotometry at 425 nm. According to Remigante et al. [35], in order to convert the absorption to $[\text{SO}_4^{2-}]$ L cells $\times 10^{-2}$, a calibrated standard curve previously obtained by precipitating known SO_4^{2-} concentrations was used. Furthermore, the rate constant (min^{-1}) was calculated by the equation: $C_t = C_\infty (1 - e^{-rt}) + C_0$, where C_t , C_∞ , and C_0 represent the intracellular SO_4^{2-} concentrations, respectively, at time t , 0, and ∞ ; e is the Neper number (2.7182818); r is the rate constant accounting for the process velocity, and t is the time fixed for each sample withdrawal. The rate constant is the time needed to reach 63% of total SO_4^{2-} intracellular concentration and $[\text{SO}_4^{2-}]$ L cells $\times 10^{-2}$ reported in figure stands for SO_4^{2-} micromolar concentration trapped by 10 mL erythrocytes (3% hematocrit).

Quantification assay of MVs by flow cytometry

In this study, we measured MVs-annexin V-positive to evaluate the PS-exposure. MVs were obtained from intact RBC after treatment with HgCl_2 . RBC were centrifuged at 2,000 g during 10 min at 4 °C [30]. After, 95 μL of supernatant containing the MVs were resuspended in 400 L of 1x binding buffer and incubated in the dark for 30 min at room temperature, with 5 L of annexin V [26]. MVs-annexin V-positive were quantified by flow cytometry. The assessment of fluorescence was performed with FACSCanto™ II, BD Biosciences, San Jose, CA, USA. For each sample, 20,000 events were recorded.

Digital holographic microscopy

The impact of HgCl_2 on RBC morphology was assessed using a Digital Holographic Microscopy (DHM® T1000 microscope) (Lyncée Tec SA, Lausanne, Switzerland) equipped with a motorized microscope stage (Märzhäuser Wetzlar GmbH & CO. KG, Wetzlar, Germany), an incubator system (LCI Live Cell Instrument, Seoul, South Korea), and a 20x/0.40 NA objective (Leica Microsystems GmbH, Wetzlar, Germany), as described in Bardyn et al. [30, 36]. DHM is a label free microscopy using a low intensive laser source limiting cell alteration. This technique is based on the quantitative measurement of the optical pathlength (OPL) delay (interferometric phase shift measurements) induced by the sample [37]. This parameter is linked to the cell volume and refractive index. The DHM images were analyzed with the software CellProfiler (Analyst) that classes the RBC in predefined morphological categories and then quantifies the different morphological types [38, 39].

As before, RBC were suspended to 10 % hematocrit and treated with HgCl_2 (10, 20 and 40 μM). Subsequently, RBC were diluted in Krebs solution and 100 μL , containing 80,000 RBCs, were seeded per well, as quadruplicates, in a 96-well black imaging plate coated with poly-L-ornithine [37]. To accelerate cell sedimentation, the plate was centrifuged (140 g for 2 min at RT).

For imaging, the plate was put under the microscope in the incubation chamber set at 37 °C and 5 % CO_2 . Four images were taken per well at 20x magnification.

Statistical analyses

Data evaluations were expressed as means \pm S.D. of three independent experiments performed in triplicate with RBC from six donors. The significance of differences was determined by one-way and two-way ANOVA followed by a Tukey's and Dunnet's multiple comparisons test. GraphPad Prism 9.1 was utilized for statistical analyses.

Results

Electrophoretic analyses of membrane proteins and Western blotting of Ankyrin and Flotillin-2 from Hg-exposed RBC

In order to explore the possible interaction of Hg with RBC membrane proteins, intact human RBC were exposed *in vitro* for 24 h in the presence of increasing HgCl_2 concentrations (10-40 μM) and the electrophoretic profiles of the membrane fraction were evaluated. The typical SDS-PAGE electrophoretic profile of RBC membrane proteins is shown in Fig. 1. Exposure of cells to all tested HgCl_2 concentrations resulted in a significant alteration in the electrophoretic profile. Therefore, with the aim of clearly identify the specific Hg-modified RBC membrane proteins, the effect of Hg on Ankyrin and Flotillin-2, proteins essential for the membrane integrity, was quantified by Western blot.

Fig. 1. SDS-PAGE analysis of total membrane proteins from Hg-treated human RBC (10, 20 and 40 μM HgCl_2) for 24 h. (A) Representative image from 9 replicate experiment of total membrane proteins. Proteins were extracted with 1 % DC buffer. Markers (MRK) (lane 1); samples from untreated RBC (CTR) (lane 2) and Hg-treated RBC (lane 3-5). (B). Location of main proteins on a total membrane protein extract.

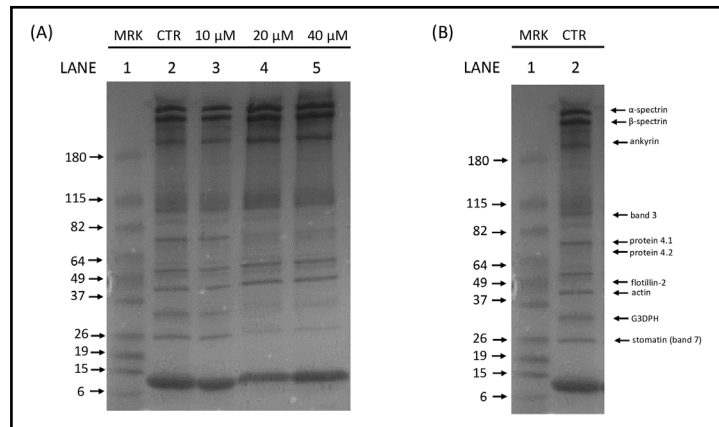


Fig. 2. Western blot analysis of Ankyrin from Hg-treated human RBC (10, 20 and 40 μM HgCl_2) for 24 h. (A) Representative analysis of a 9 replicate experiment. Western blot lanes. Sample from untreated (CTR) (lane 1) and Hg-treated RBC (lane 2-4). (B) Corresponding densitometric analyses expressed as the mean \pm SD (n=9). Statistical analysis was performed with one-way ANOVA followed by Tukey's test. *** (p<0.001) and * (p<0.05) indicate a significant difference from CTR, ### (p<0.001) and ## (p<0.01) indicate a significant difference from 10 μM .

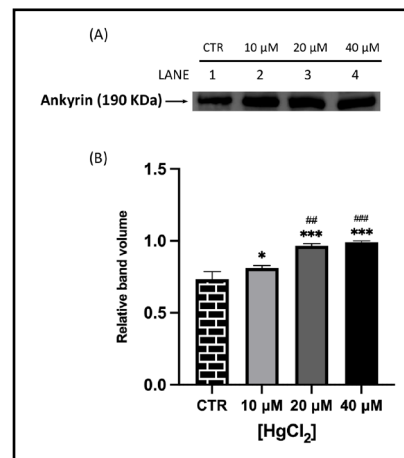


Fig. 3. Western blot analysis of Flotillin-2 from Hg-treated human RBC (10, 20 and 40 μM HgCl_2) for 24 h. (A) Representative analysis of a 9 replicate experiment. Western blot lanes. Sample from untreated (CTR) (lane 1) and Hg-treated RBC (lane 2-4). (B) Corresponding densitometric analyses expressed as the mean of the means \pm SD (n=9). Statistical analysis was performed with one-way ANOVA followed by Tukey's test. *** (p<0.001) indicate a significant difference from CTR and ns (p > 0.05) indicate no significant difference from CTR. ### (p<0.001) indicate a significant difference from 10 μM , and §§§ (p<0.001) indicate a significant difference from 20 μM .

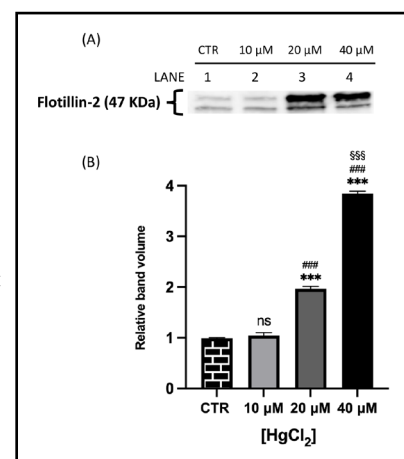


Fig. 2 and 3 show that both proteins of interest, Ankyrin and Flotillin-2, were detected at their molecular weights (190 and 47 kDa, respectively). Their amounts significantly increased after overnight Hg-treatment (range 10-40 μM) in contrast to those in untreated cells (CTR). In particular, Ankyrin showed an increase in a dose-dependent manner, with a significant effect starting at concentrations as low as 10 μM and reached a plateau after 20 μM . As for Flotillin-2, the addition of HgCl_2 10 μM had no effect whereas fold-changes of 2 and 4 were observed for 20 and 40 μM , respectively.

Effect of mercury on sulphate uptake in RBC

B3p-Ankyrin binding appears to be crucial for the proper functioning of both proteins. Consequently, the effect of Hg on the ionic transport function of B3p was analyzed. The efficiency of B3p can be monitored by determining the rate constant for SO_4^{2-} uptake, which is slower and more easily detectable than Cl^- or HCO_3^- uptake. SO_4^{2-} uptake kinetics (as a measure of the level of anion transport) in RBC treated with different concentrations of HgCl_2 (10, 20 and 40 μM) or with the B3p inhibitor DIDS (10 μM) are shown in Fig. 4. All treatments significantly reduced the uptake rate of SO_4^{2-} compared with controls. In addition, RBC treated with DIDS showed similar degrees of saturation. It clearly indicates that Hg inhibited the B3p transport function.

Effect of Hg on PS-bearing MVs release from RBC

PS externalization on MVs were identified based on binding to annexin-V. It is known that increased MVs exposing PS are involved in prothrombotic effects [40–42].

As illustrated in Fig. 5, differences in PS exposure on MVs membrane were observed. In particular, we observed a dose-dependent exposure, consequently, Hg at higher concentrations also supports PS exposure in MVs.

Effect of mercury on RBC morphology

Cell morphology was observed using DHM imaging. Fig. 6 shows the effect of HgCl_2 on RBC morphology after 24 hours of incubation at 37 °C. The proportion of different morphological RBC types with respect to the total RBC populations presented in Fig. 6 (A). Seven RBC shape types were identified (see Fig. 6B) and classified as follows: discocytes, corresponding to the physiological shape; stomatocytes, echinocytes I, II and III (intermediate transition between discocytes and spherocytes characterised by the presence of a respectively increasing number of spicules), and the last stage of RBC aging sphero-echinocytes and spherocytes.

Fig. 4. SO_4^{2-} uptake measurement. Time course of SO_4^{2-} uptake in untreated (CTR) RBC or Hg-treated human RBC (10, 20 and 40 μM HgCl_2) for 4 h after different times of incubation or with DIDS. Data correspond to the means \pm SD (n=9). Statistical analysis was performed with two-way ANOVA followed by Dunnet's post test. *** (p<0.001) indicates a significant difference from CTR.

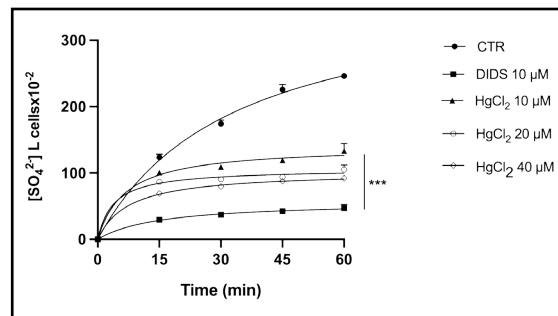
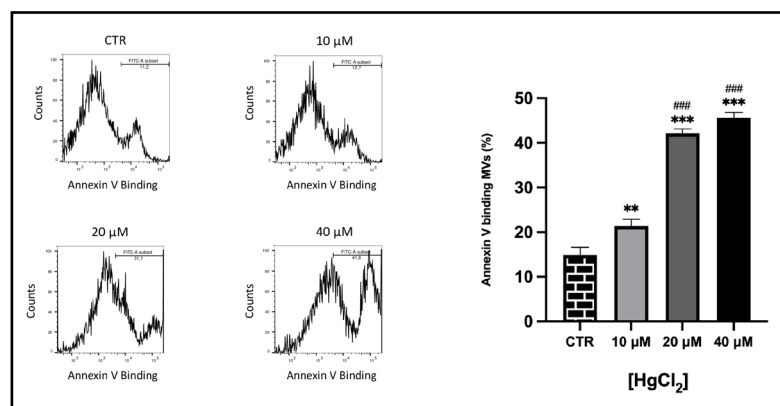


Fig. 5. Effect of Hg-induced PS exposure in MVs. RBC were treated with HgCl_2 (10, 20 and 40 μM) for 24 h and PS exposure was evaluated via Annexin-V-binding. Data correspond to the means \pm SD (n=9). (A) Original histogram of CTR and Hg-treatment. (B) Histogram of Hg-treated cells. Statistical analysis was performed with one-way ANOVA followed by Tukey's test. *** (p<0.001) and ** (p<0.01) indicate a significant difference from control (CTR), ### (p<0.001) indicate a significant difference from 10 μM .



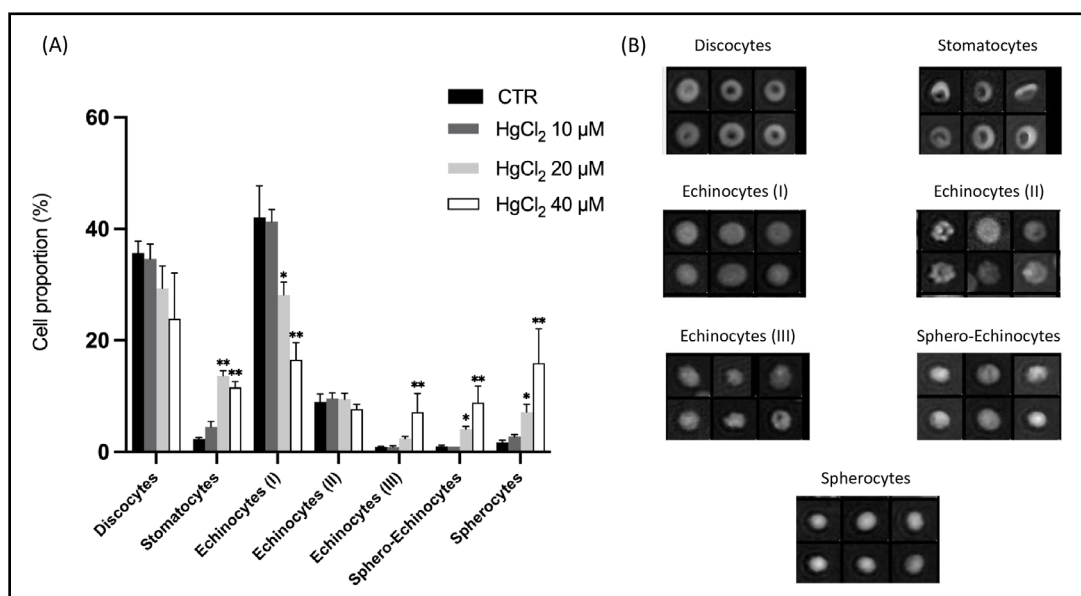


Fig. 6. Effect of different concentrations of HgCl₂ (10, 20 and 40 μM) for 24 h on RBC morphology. (A) Analysis of RBC morphology. Data correspond to the means ± SD (n=9). Statistical analysis was performed with two-way ANOVA followed by Tukey's test. ** (p<0.01) and * (p<0.05), indicates significant difference compared to CTR. (B) Illustrative phase images showing morphological changes of RBC acquired by digital DHM.

As a global trend after 24 h of incubation, the addition of HgCl₂ induced decreases of discocytes from 35 (CTR) to 24% (HgCl₂ 40 μM) and echinocytes (I) from 42 to 16.5% and concomitant increases of echinocytes (III) from 0.9 to 7.1%, sphero-echinocytes from 1 to 8.9% and spherocytes from 1.7 to 16%; as for the echinocytes (II) no difference was observed between all conditions. It highlights a clear shift from reversible to irreversible morphologies. Moreover, the 10 μM had a moderate effect, whereas the addition of 40 μM of HgCl₂ significantly affected the RBC.

Discussion

In recent years, Hg toxicity received considerable scientific attention because of potential health and environmental risks of this widespread environmental pollutant [43]. The toxic biological effects of human exposure to this heavy metal are extremely numerous, affecting different organs and tissues. Among the molecular mechanisms underlying Hg toxicity, protein interactions seem to play a key role, possibly leading to structural and functional alterations, thus interfering with important metabolic as well as regulatory cellular functions [44].

RBC are particularly vulnerable to the harmful effects of Hg [45], being a preferential store for this heavy metal. Hg accumulates in these cells mainly bound to the SH group of the thiol of glutathione present in very high concentrations in these cells [46]. As far as the Hg-Hb interaction is concerned, we recently reported the presence of proteins with reduced electrophoretic mobility compared to that corresponding to the Hb monomer, upon cell incubation with HgCl₂. In particular, a protein band likely corresponding to a Hb tetramer, on the basis of its apparent MW, was observable [27].

In this study, the effect of HgCl₂ on RBC membrane proteins was evaluated. Intact human RBC were exposed to HgCl₂ *in vitro* and we demonstrated that this treatment induced significant alterations in the electrophoretic behavior of membrane proteins, including proteins from the cytoskeleton, the flexible network anchored to the cell membrane. As amply reported in literature, several membrane proteins possess SH groups, critical in maintaining

the protein folding, and the correct interaction between cytoskeletal proteins and integral proteins [47]. A significant depletion in the overall membrane thiols has been reported in our previous paper, in similar experimental conditions [27]. In addition, data presented in this paper from Western blot analysis clearly identified significant modifications of specific membrane proteins, including Ankyrin and Flotillin-2.

Ankyrin is a major protein responsible for connecting plasma membrane to the underlying cytoskeleton [28]. Specifically, ankyrin is an anchor protein, which tethers the β subunit of Spectrin to the cytoplasmic domain of B3p. The formation of this linkage is essential to maintain the integrity of the plasma membrane. Specific Cys residues are critical for this anchoring and their derivatization with thiol reagents blocks the interaction between both proteins [47]. Moreover, possible Hg interaction with these binding sites can be hypothesized inducing conformational changes in these membrane proteins [48–50]. Since an accumulation of ankyrin was observed following the addition of Hg, it could be hypothesized that the presence of Hg does not induce a release of ankyrin from the membrane but a change in binding site. This modification could alter protein-protein interactions, especially on the B3p dimer-ankyrin complex, leading to morphological changes.

Of particular interest are the data from Flotillin-2, a major protein of lipid raft that contributes the organization of functional domains [29, 51, 52]. Therefore, the effect of Hg treatment on this protein was analyzed by Western blot. Again, a significant alteration protein binding was observed. Hg, interacting with thiol groups, could alter the interaction of these proteins with the membrane and the interaction between the proteins themselves. It leads to significant changes in the lateral organization of the plasma membrane. Specifically, proper membrane anchoring of these proteins requires the formation of a thioester bond between a cysteine residue and palmitic acid. In addition, palmitoylation may facilitate interactions of Flotillins with other S-palmitoylated proteins residing in lipid rafts, such as palmitoylated scaffold membrane protein 1 (MPP1) [53, 54]. Flotillin-2 was also reported to bind on B3p complex during the storage of RBCs but without an accumulation on the whole membrane, suggesting a migration of flotillin-2 [31]. The modification in lipid-raft organization because of RBC storage lesions [55] could be triggered here by the presence of Hg. It may also play a role in storage-induced microvesiculation [31, 56], which corroborates with the reported data.

Therefore, Hg treatment could lead to significant alteration of cell shape. Accordingly, analysis with the digital holographic microscope indicates the Hg-exposure induced dramatic changes in biconcave discoid RBC morphology, resulting in significant increase in the number of stomatocytes and spherocytes upon Hg treatment. The alteration of RBC morphology associated with PS-bearing MVs formation. The modification in membrane protein organizations triggered by Hg could explain the morphology shift from discocytes to spherocytes. However, additional experiments will be required to decipher the mechanisms behind such morphological alteration. Indeed, it could be both/either due by a rupture of the B3p-ankyrin binding (without release of ankyrin from the membrane) and/or from the flip-flop of PS [57] due to Hg-induced stress.

In addition of the direct effect of Hg on Cys residues and protein structure and organization, calcium intake can play a role. Indeed, it is well known that Hg toxicity is associated with increased intracellular calcium [19, 58]. Calcium influx is responsible of several cell modifications [9, 59], leading to eryptosis [60, 61], and is associated to loss of physiological membrane asymmetry due to PS exposure to the external membrane leaflet, and to the release of MVs [61–63]. In this respect, changes in lipid asymmetry may affect the membrane stability, thus representing an additional mechanism in Hg-induced MVs biosynthesis [62]. Accordingly, in this study, we observed for the first time that Hg cell treatment induces formation of MVs exposing PS. These findings may confirm the harmful effects of Hg in CVD, as PS-expressing MVs are known to possess increased pro-coagulant activity [40, 64], providing a catalytic surface promoting the assembly of the enzyme complex of the coagulation cascade and therefore actively contributing to thrombus formation.

Altogether, the findings reported in this paper provide new insight in the Hg-induced protein modification in human RBC affecting the complex biological system of cellular membrane. Our work represents the first study revealing Hg-induced alterations of specific membrane proteins, such as Ankyrin and Flotillin-2, that could be responsible of decrease membrane stability. In particular, Hg could induce dismantle of vertical cohesion between the plasma membrane and cytoskeleton as well as destabilization of lateral linkages of functional domains. As a consequence, decreased membrane deformability could impair RBC capacity to deal with the shear forces in the circulation increasing membrane fragmentation.

Furthermore, findings described in this paper have also significant implication in RBC physiology, particularly related with the B3p anion exchanger, that we report to reduce its activity upon Hg treatment in a dose dependent manner. B3p, indeed, is also endowed with specific anion exchange capabilities, whose activity is essential for the maintenance of ionic balance [65]. In particular, the main function of this protein is the transport of $\text{Cl}^-/\text{HCO}_3^-$; a fundamental process in the steps leading to the excretion of CO_2 in the lungs [66]. B3p also regulates the metabolism of RBC. In fact, the N-terminal domain is also capable of binding numerous glycolytic enzymes, diverting the glucose metabolism towards the phosphate pentose pathway, when the cell is saturated with oxygen [67]. Indeed, several transporters and channels, among which the B3p is of particular importance, regulate normal water content in RBC. Alterations in the regulation of cation homeostasis impair the ability of RBC to maintain normal cell volume, which in turn causes a decrease in cell deformability and thus compromises optimal oxygen delivery [68] and nitric oxide (NO) exchanges. As previously reported, Hg-modified Hb could be altered in its binding to NO [27]. Indeed, two critical Cys in position 93 of the beta-chains have been identified as NO ligand [69], playing a role in Hb-mediated NO release. Alteration of these Cys, following Hg interaction, might impair the Hb-mediated regulation of blood flow, therefore representing one of the physiologically important manifestations of Hg poisoning in these cells [27].

Finally, these observations and literature data point to RBC as important target of Hg poisoning following human exposure to this heavy metal [61, 70]. In this context, nutritional components including vitamins and antioxidant polyphenols, normally present in our diet, have potential to modulate Hg toxicity [71, 72], therefore representing ideal candidates for nutritional/nutraceutical strategies to counteract the clinical outcomes of chronic Hg exposure in humans.

Acknowledgements

Author Contributions

R.N. (methodology; investigation; visualization; review and editing). E.L. (writing—original draft preparation; review and editing; data curation). P.P. (software; investigation; writing—original draft preparation). D.C. (software; formal analysis). M.P. (validation; writing—review and editing; supervision; visualization). C.M. (Conceptualization; validation; writing—review and editing; supervision).

Funding Sources

E.L. received financial supports from The SRTS VD foundation.

Statement of Ethics

Informed consent was obtained from all subjects involved in the study.

Disclosure Statement

The authors have no conflicts of interest to declare.

References

- 1 Rice KM, Walker EM, Wu M, Gillette C, Blough ER: Environmental mercury and its toxic effects. *J Prev Med Public Health* 2014;47:74–83.
- 2 Spiegel SJ: New mercury pollution threats: a global health caution. *Lancet* 2017;390:226–227.
- 3 Qiu YW, Wang WX: Comparison of mercury bioaccumulation between wild and mariculture food chains from a subtropical bay of Southern China. *Environ Geochem Health* 2016;38:39–49.
- 4 McKelvey W, Gwynn RC, Jeffery N, Kass D, Thorpe LE, Garg RK, Palmer CD, Parsons PJ: A biomonitoring study of lead, cadmium, and mercury in the blood of New York city adults. *Environ Health Perspect* 2007;115:1435–1441.
- 5 Aschner M, Carvalho C: The biochemistry of mercury toxicity. *Biochim Biophys Acta Gen Subj* 2019;1863:129412.
- 6 Yang L, Zhang Y, Wang F, Luo Z, Guo S, Strähle U: Toxicity of mercury: Molecular evidence. *Chemosphere* 2020;245:125586.
- 7 Zalups RK: Molecular interactions with mercury in the kidney. *Pharmacol Rev* 2000;52:113–143.
- 8 Oz SG, Tozlu M, Yalcin SS, Sozen T, Guven GS: Mercury vapor inhalation and poisoning of a family. *Inhal Toxicol* 2012;24:652–658.
- 9 Notariale R, Perrone P, Mele L, Lettieri G, Piscopo M, Manna C: Olive Oil Phenols Prevent Mercury-Induced Phosphatidylserine Exposure and Morphological Changes in Human Erythrocytes Regardless of Their Different Scavenging Activity. *Int J Mol Sci* 2022;23:5693.
- 10 Lettieri G, Notariale R, Carusone N, Giarra A, Trifuoggi M, Manna C, Piscopo M: New Insights into Alterations in PL Proteins Affecting Their Binding to DNA after Exposure of *Mytilus galloprovincialis* to Mercury-A Possible Risk to Sperm Chromatin Structure? *Int J Mol Sci* 2021;22:5893.
- 11 Houston MC: The Role of Mercury in Cardiovascular Disease. *J Cardiovasc Dis Diagn* 2014;2:5.
- 12 Yilmaz OH, Karakulak UN, Tutkun E, Bal C, Gunduzoz M, Ercan Onay E, Ayturk M, Tek Ozturk M, Alaguney ME: Assessment of the Cardiac Autonomic Nervous System in Mercury-Exposed Individuals via Post-Exercise Heart Rate Recovery. *Med Princ Pract* 2016;25:343–349.
- 13 Fernandes Azevedo B, Barros Furieri L, Peçanha FM, Wiggers GA, Frizera Vassallo P, Ronacher Simões M, Fiorim J, Rossi de Batista P, Fiorese M, Rossoni L, Stefanon I, Alonso MJ, Salaices M, Valentim Vassallo D: Toxic effects of mercury on the cardiovascular and central nervous systems. *J Biomed Biotechnol* 2012;2012:949048.
- 14 Wierzbicki R, Prażanowski M, Michalska M, Krajewska U, Mielicki WP: Disorders in blood coagulation in humans occupationally exposed to mercuric vapors. *J Trace Elem Exp Med* 2002;15:21–29.
- 15 Notariale R, Infantino R, Palazzo E, Manna C: Erythrocytes as a Model for Heavy Metal-Related Vascular Dysfunction: The Protective Effect of Dietary Components. *Int J Mol Sci* 2021;22:6604.
- 16 Ferreira G, Santander A, Chavarría L, Cardozo R, Savio F, Sobrevia L, Nicolson GL: Functional consequences of lead and mercury exposomes in the heart. *Mol Aspects Med* 2021;101048.
- 17 Genchi G, Sinicropi MS, Carocci A, Lauria G, Catalano A: Mercury Exposure and Heart Diseases. *Int J Environ Res Public Health* 2017;14:74.
- 18 Clarkson TW, Magos L, Myers GJ: The toxicology of mercury--current exposures and clinical manifestations. *N Engl J Med* 2003;349:1731–1737.
- 19 Lim KM, Kim S, Noh JY, Kim K, Jang WH, Bae ON, Chung SM, Chung JH: Low-Level Mercury Can Enhance Procoagulant Activity of Erythrocytes: A New Contributing Factor for Mercury-Related Thrombotic Disease. *Environ. Health Perspect* 2010;118:928–935.
- 20 Akagi H, Malm O, Branches FJP, Kinjo Y, Kashima Y, Guimaraes JRD, Oliveira RB, Haraguchi K, Pfeiffer WC, Takizawa Y, Kato H: Human exposure to mercury due to gold mining in the Tapajos river basin, Amazon, Brazil. Speciation of mercury in human hair, blood and urine; in Porcella DB, Huckabee JW, Weatley B (eds): *Mercury as a Global Pollutant*. Springer, Dordrecht, 1995. DOI: 10.1007/978-94-011-0153-0_10.
- 21 Rajae M, Sánchez BN, Renne EP, Basu N: An Investigation of Organic and Inorganic Mercury Exposure and Blood Pressure in a Small-Scale Gold Mining Community in Ghana. *Int J Environ Res Public Health* 2015;12:10020–10038.
- 22 Haybar H, Shahrabi S, Rezaeeyan H, Shirzad R, Saki N: Endothelial Cells: From Dysfunction Mechanism to Pharmacological Effect in Cardiovascular Disease. *Cardiovasc Toxicol* 2019;19:13–22.

- 23 Litvinov RI, Weisel JW: Role of red blood cells in haemostasis and thrombosis. *ISBT Sci Ser* 2017;12:176–183.
- 24 Fischer D, Büsow J, Meybohm P, Weber CF, Zacharowski K, Urbschat A, Müller MM, Jennewein C: Microparticles from stored red blood cells enhance procoagulant and proinflammatory activity. *Transfusion* 2017;57:2701–2711.
- 25 Thangaraju K, Neerukonda SN, Katneni U, Buehler PW: Extracellular Vesicles from Red Blood Cells and Their Evolving Roles in Health, Coagulopathy and Therapy. *Int J Mol Sci* 2021;22:153.
- 26 Chiva-Blanch G, Sala-Vila A, Crespo J, Ros E, Estruch R, Badimon L: The Mediterranean diet decreases prothrombotic microvesicle release in asymptomatic individuals at high cardiovascular risk. *Clin Nutr* 2020;39:3377–3384.
- 27 Piscopo M, Notariale R, Tortora F, Lettieri G, Palumbo G, Manna C: Novel Insights into Mercury Effects on Hemoglobin and Membrane Proteins in Human Erythrocytes. *Molecules* 2020;25:3278.
- 28 Lux SE: Anatomy of the red cell membrane skeleton: unanswered questions. *Blood* 2016;127:187–199.
- 29 Salzer U, Prohaska R: Stomatin, flotillin-1, and flotillin-2 are major integral proteins of erythrocyte lipid rafts. *Blood* 2001;97:1141–1143.
- 30 Bardyn M, Rappaz B, Jaferzadeh K, Crettaz D, Tissot JD, Moon I, Turcatti G, Lion N, Prudent M: Red blood cells ageing markers: a multi-parametric analysis. *Blood Transfus* 2017;15:239–248.
- 31 Prudent M, Delobel J, Hübner A, Benay C, Lion N, Tissot JD: Proteomics of Stored Red Blood Cell Membrane and Storage-Induced Microvesicles Reveals the Association of Flotillin-2 With Band 3 Complexes. *Front Physiol* 2018;9:421.
- 32 Delobel J, Prudent M, Tissot JD, Lion N: Proteomics of the red blood cell carbonylome during blood banking of erythrocyte concentrates. *Proteomics Clin Appl* 2016;10:257–266.
- 33 Romano L, Passow H: Characterization of anion transport system in trout red blood cell. *Am J Physiol Cell Physiol* 1984;246:C330–C338.
- 34 Jessen F, Sjöholm C, Hoffmann EK: Identification of the anion exchange protein of ehrlich cells: A kinetic analysis of the inhibitory effects of 4,4'-diisothiocyano-2,2'-stilbene-disulfonic acid (DIDS) and labeling of membrane proteins with 3H-DIDS. *J Membr Biol* 1986;92:195–205.
- 35 Remigante A, Spinelli S, Basile N, Caruso D, Falliti G, Dossena S, Marino A, Morabito R: Oxidation Stress as a Mechanism of Aging in Human Erythrocytes: Protective Effect of Quercetin. *Int J Mol Sci* 2022;23:7781.
- 36 Rappaz B, Barbul A, Emery Y, Korenstein R, Depeursing C, Magistretti PJ, Marquet P: Comparative study of human erythrocytes by digital holographic microscopy, confocal microscopy, and impedance volume analyzer. *Cytometry Part A* 2008;73:895–903.
- 37 Bardyn M, Allard J, Crettaz D, Rappaz B, Turcatti G, Tissot JD, Prudent M: Image- and Fluorescence Based Test Shows Oxidant-Dependent Damages in Red Blood Cells and Enables Screening of Potential Protective Molecules. *Int J Mol Sci* 2021;22:4293.
- 38 Carpenter AE, Jones TR, Lamprecht MR, Clarke C, Kang IH, Friman O, Guertin DA, Chang JH, Lindquist RA, Moffat J, Golland P, Sabatini DM: CellProfiler: image analysis software for identifying and quantifying cell phenotypes. *Genome Biol* 2006;7:100.
- 39 Jones TR, Carpenter AE, Lamprecht MR, Moffat J, Silver SJ, Grenier JK, Castoreno AB, Eggert US, Root DE, Golland P, Sabatini DM: Scoring diverse cellular morphologies in image-based screens with iterative feedback and machine learning. *Proc Natl Acad Sci U S A* 2009;106:1826–1831.
- 40 Rubin O, Delobel J, Prudent M, Lion N, Kohl K, Tucker EI, Tissot JD, Angelillo-Scherrer A: Red blood cell-derived microparticles isolated from blood units initiate and propagate thrombin generation. *Transfusion* 2013;53:1744–1754.
- 41 Jy W, Johansen ME, Bidot C, Horstman LL, Ahn YS: Red cell-derived microparticles (RMP) as haemostatic agent. *Thromb Haemost* 2013;110:751–760.
- 42 Zecher D, Cumpelik A, Schifferli JA: Erythrocyte-derived microvesicles amplify systemic inflammation by thrombin-dependent activation of complement. *Arterioscler Thromb Vasc Biol* 2014;34:313–320.
- 43 Yousaf B, Amina, Liu G, Wang R, Imtiaz M, Rizwan MS, Zia-Ur-Rehman M, Qadir A, Si Y: The importance of evaluating metal exposure and predicting human health risks in urban–periurban environments influenced by emerging industry. *Chemosphere* 2016;150:79–89.
- 44 Ynalvez R, Gutierrez J, Gonzalez-Cantu H: Mini-review: toxicity of mercury as a consequence of enzyme alteration. *Biomaterials* 2016;29:781–788.

- 45 Ahmad S, Mahmood R: Mercury chloride toxicity in human erythrocytes: enhanced generation of ROS and RNS, hemoglobin oxidation, impaired antioxidant power, and inhibition of plasma membrane redox system. *Environ Sci Pollut Res Int* 2019;26:5645–5657.
- 46 Hernández LE, Sobrino-Plata J, Montero-Palmero MB, Carrasco-Gil S, Flores-Cáceres ML, Ortega-Villasante C, Escobar C: Contribution of glutathione to the control of cellular redox homeostasis under toxic metal and metalloid stress. *J Exp Bot* 2015;66:2901–2911.
- 47 Thevenin BJM, Willardson BM, Low PS: The Redox State of Cysteines 201 and 317 of the Erythrocyte Anion Exchanger Is Critical for Ankyrin Binding. *J Biol Chem* 1989;264:15886–15892.
- 48 Willardson BM, Thevenin BJ, Harrison ML, Kuster WM, Benson MD, Low PS: Localization of the ankyrin-binding site on erythrocyte membrane protein, band 3. *J Biol Chem* 1989;264:15893–15899.
- 49 Bennett V, Stenbuck PJ: The membrane attachment protein for spectrin is associated with band 3 in human erythrocyte membranes. *Nature* 1979;280:468–473.
- 50 Grey JL, Kodippili GC, Simon K, Low PS: Identification of contact sites between ankyrin and band 3 in the human erythrocyte membrane. *Biochemistry* 2012;51:6838–6846.
- 51 Akkaya B, Kucukal E, Little JA, Gurkan UA: Mercury leads to abnormal red blood cell adhesion to laminin mediated by membrane sulfatides. *Biochim Biophys Acta Biomembr* 2019;1861:1162–1171.
- 52 Kwiatkowska K, Matveichuk OV, Fronk J, Ciesielska A. Flotillins: At the Intersection of Protein S-Palmitoylation and Lipid-Mediated Signaling. *Int J Mol Sci* 2020;21:2283.
- 53 Biernatowska A, Podkalicka J, Majkowski M, Hryniewicz-Jankowska A, Augoff K, Kozak K, Korzeniewski J, Sikorski AF: The role of MPP1/p55 and its palmitoylation in resting state raft organization in HEL cells. *Biochim Biophys Acta* 2013;1833:1876–1884.
- 54 Biernatowska A, Augoff K, Podkalicka J, Tabaczar S, Gajdzik-Nowak W, Czogalla A, Sikorski AF: MPP1 directly interacts with flotillins in erythrocyte membrane - Possible mechanism of raft domain formation. *Biochim Biophys Acta Biomembr* 2017;1859:2203–2212.
- 55 Yoshida T, Blair A, D'alessandro A, Nemkov T, Dioguardi M, Silliman CC, Dunham A: Enhancing uniformity and overall quality of red cell concentrate with anaerobic storage. *Blood Transfus* 2017;15:172–181.
- 56 Salzer U, Zhu R, Luten M, Isobe H, Pastushenko V, Perkmann T, Hinterdorfer P, Bosman GJ: Vesicles generated during storage of red cells are rich in the lipid raft marker stomatin. *Transfusion* 2008;48:451–462.
- 57 Gov N, Cluitmans J, Sens P, Bosman GJCGM: Chapter 4 Cytoskeletal Control of Red Blood Cell Shape: Theory and Practice of Vesicle Formation. *APLBL* 2009;95–119.
- 58 Jomova K, Valko M. Mercury Toxicity, in Kretsinger RH, Uversky VN, Permyakov EA (eds): *Encyclopedia of Metalloproteins*. New York, Springer, 2013, pp 1367–1372.
- 59 Flatt JF, Bawazir WM, Bruce LJ: The involvement of cation leaks in the storage lesion of red blood cells. *Front Physiol* 2014;5:214.
- 60 Föller M, Lang F: Ion Transport in Eryptosis, the Suicidal Death of Erythrocytes. *Front Cell Dev Biol* 2020;8:597.
- 61 Officioso A, Alzoubi K, Lang F, Manna C: Hydroxytyrosol inhibits phosphatidylserine exposure and suicidal death induced by mercury in human erythrocytes: Possible involvement of the glutathione pathway. *Food Chem Toxicol* 2016;89:47–53.
- 62 Manno S, Takakuwa Y, Mohandas N: Identification of a functional role for lipid asymmetry in biological membranes: Phosphatidylserine-skeletal protein interactions modulate membrane stability. *Proc Natl Acad Sci U S A* 2002;99:1943–1948.
- 63 Prudent M, Tissot JD, Lion N: *In vitro* assays and clinical trials in red blood cell aging: Lost in translation. *Transfus Apher Sci* 2015;52:270–276.
- 64 Shustova ON, Antonova OA, Golubeva NV, Khaspekova SG, Yakushkin VV, Aksuk SA, Alchinova IB, Karganov MY, Mazurov AV: Differential procoagulant activity of microparticles derived from monocytes, granulocytes, platelets and endothelial cells: impact of active tissue factor. *Blood Coagul. Fibrinolysis* 2017;28:373–382.
- 65 Morabito R, Remigante A, Spinelli S, Vitale G, Trichilo V, Loddo S, Marino A: High Glucose Concentrations Affect Band 3 Protein in Human Erythrocytes. *Antioxidants* 2020;9:365.
- 66 Jennings ML: Cell physiology and molecular mechanism of anion transport by erythrocyte band 3/AE1. *Am J Physiol Cell Physiol* 2021;321:1028–1059.
- 67 Low PS, Rathinavelu P, Harrison ML: Regulation of glycolysis via reversible enzyme binding to the membrane protein, band 3. *J Biol Chem* 1993;268:14627–14631.

- 68 Brugnara C: Erythrocyte membrane transport physiology. *Curr Opin Hematol* 1997;4:122–127.
- 69 Gladwin MT, Lancaster JR, Freeman BA, Schechter AN: Nitric oxide's reactions with hemoglobin: a view through the SNO-storm. *Nat Med* 2003;9:496–500.
- 70 Tagliaferro L, Officioso A, Sorbo S, Basile A, Manna C: The protective role of olive oil hydroxytyrosol against oxidative alterations induced by mercury in human erythrocytes. *Food Chem Toxicol* 2015;82:59–63.
- 71 Tortora F, Notariale R, Lang F, Manna C: Hydroxytyrosol Decreases Phosphatidylserine Exposure and Inhibits Suicidal Death Induced by Lysophosphatidic Acid in Human Erythrocytes. *Cell Physiol Biochem* 2019;53:921–932.
- 72 Tortora F, Notariale R, Maresca V, Good KV, Sorbo S, Basile A, Piscopo M, Manna C: Phenol-Rich Feijoa sellowiana (Pineapple Guava) Extracts Protect Human Red Blood Cells from Mercury-Induced Cellular Toxicity. *Antioxidants* 2019;8:220.